

## COMPARATIVE STUDY ON MICROMECHANICAL PROPERTIES OF ZnO:Ga AND ZnO:In LUMINESCENT CERAMICS

F. Muktepavela<sup>1,\*</sup>, A. Zolotarjovs<sup>1</sup>, R. Zabels<sup>1</sup>, K. Kundzins<sup>1</sup>,  
E. Gorokhova<sup>2</sup>, E. Tamanis<sup>3</sup>

<sup>1</sup>Institute of Solid State Physics, University of Latvia,  
8 Kengaraga Str., Riga, LV-1063, LATVIA

<sup>2</sup>Scientific and Production Association S.I.Vavilov State Optical Institute,  
36 Babushkina Str., Saint Petersburg, 192171, RUSSIA

<sup>3</sup>Daugavpils University,  
1 Parades Str., Daugavpils, LV-5401, LATVIA  
\*e-mail: famuk@latnet.lv

Indium (0.038 at.%) and gallium (0.042 at.%) doped ZnO ceramics were prepared by hot pressing. Ceramics were investigated to determine their structural and mechanical characteristics for the prospective use in scintillators. Based on results of nanoindentation, atom force and scanning electron microscopy as well as energy dispersive X-ray spectra measurements, locations of gallium within grain, indium at grain boundaries (GBs) and their different effect on the mechanical properties of ZnO ceramics were detected. Doping of gallium led to the increased modulus of elasticity in grain, decreased hardness near GBs, stabilization of micropores and brittle intercrystalline fracture mode. ZnO:In ceramic has modulus of elasticity and hardness values close to ZnO characteristics, the increased fracture toughness and some plasticity near GBs. Differences in the micromechanical properties of the ceramics correlate with the location of dopants. Results demonstrate that the ZnO:In ceramic has a greater stress relaxation potential than the ZnO:Ga.

**Keywords:** Hot pressed ZnO ceramics, microstructure, nanoindentation, fracture mode.

## 1. INTRODUCTION

---

ZnO as a wide-band-gap (band gap of 3.37 eV) multifunctional semiconductor possesses excellent luminescent characteristics and is a promising material for scintillators [1]–[3]. With the recent advances in hot press sintering technology, transparent ZnO ceramics based on nanopowders have aroused great interest for the use in fast and high-efficient photo- or X-ray luminescence scintillators [4]. Addition of donor dopants such as Ga or In leads to the improved scintillation characteristics of the ZnO ceramics [5]–[8]. However, the location of dopants in the microstructure is not yet clear. Moreover, despite many studies on the structural and optical properties of the doped ZnO:Ga and ZnO: In ceramics [8], [9], their mechanical characteristics remain practically unexplored even though the modern technology imposes rather strict requirements towards the mechanical properties of brittle optical components as they are subject to vibrations, small mechanical and thermal shock loads. The lack of comparative data on

mechanical properties makes it difficult to use these ceramics. Furthermore, mechanical properties are highly structure sensitive [10] and, thus, they can determine not only the technological properties of ceramics, but also the influence of doped elements on the structural-phase state of ceramics. In this regard, as a fast and accurate method to measure the modulus of elasticity and hardness, nanoindentation (NI) is most applicable to ZnO ceramics (in form of thin discs) [11], [12]. NI has been successfully used to detect the mechanical properties of ZnO thin films, single crystals, ceramics and the role of GBs in the fine dispersion materials [13]–[16].

In the present research, the structure, hardness, modulus of elasticity as well as the fracture mode of Ga- (0.042 at.%) and In (0.038 at.%) doped ZnO ceramics are investigated. The aim of the study is to determine the location of dopants in the microstructure of ceramics.

## 2. EXPERIMENTAL

---

Commercial zinc oxide powder (Sigma-Aldrich, USA) was used to obtain ceramics. The indium and gallium were introduced in the form of  $\text{In}_2\text{O}_3$  and  $\text{Ga}_2\text{O}_3$  by mechanical mixing with the original ZnO powder during 40 min at 293 K [8], [9]. The level of dopants was chosen based on previously studies [9] and corresponded to practically the same scintillation properties of In- and Ga-doped ZnO ceramics. The undoped ZnO, Ga-, and In-doped ZnO ceramics were fabricated by hot uniaxial pressing under vacuum conditions at 1150 °C, 200 MPa for 60 min [4], [9]. The transparent ceramics have been shaped into discs with

a diameter of 20–25 mm and a thickness of 1.0–1.5 mm after mechanical processing. The microstructures of etched ceramics surfaces and fracture modes were studied using optical (Nikon, Eclipse L150), atom force AFM (VEECO CP-II) and scanning electron microscopy SEM (TESCAN Lyra 3) equipped with an energy dispersive X-ray spectrometer EDS (Oxford, AZ tec). The nanoindentation station (MTS Nano G200) equipped with a Berkovich-type diamond indenter tip (radius < 20 nm) was used for direct continuous stiffness measuring (CSM), registration of load and displacement, as well as topography imaging.

## 3. RESULTS AND DISCUSSION

### 3.1. Microstructure of Ceramics

Figure 1 shows the microstructures of the undoped, Ga-, and In-doped ZnO ceramics. The microstructure of undoped ZnO ceramics (Fig. 1a) consists of grains with the grain size of 10–25  $\mu\text{m}$ . The addition of Ga and In changes the microstructure of activated ceramics.

Gallium leads to the decrease of the grain size (3–8  $\mu\text{m}$ ) without changing the shape of GBs, they remain straight and faceted in places (Fig. 1b, c).

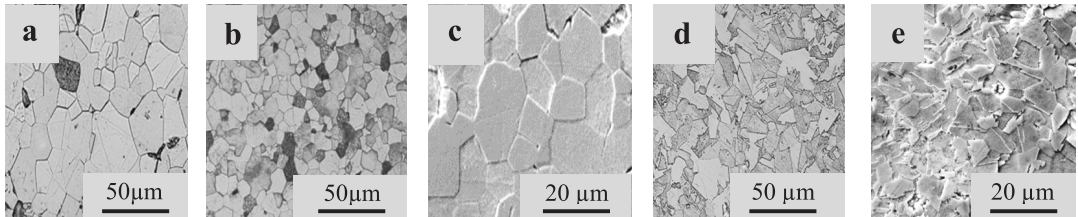


Fig. 1. Optical (a, b, d) and SEM(c, e) images of etched external surfaces of undoped (a), Ga-doped (b, c), and In-doped (d, e) ZnO ceramics.

Indium alters the microstructure more significantly than gallium (Fig. 1d, e) changing the shape of both grains and GBs: fine grains are irregular, elongated, some faceted grains have size of 8–12  $\mu\text{m}$ , and a serrated shape of GBs appears. A similar influence of indium on the GBs shape in the

ZnO ceramics based on different ZnO powders was described in [8]. Faceted straight GBs for the mechanical properties are the paths for the easy propagation of cracks. However, the presence of the serrated GBs in the ZnO:In ceramics prevents the rapid spread of cracks along GBs [10].

### 3.2. Nanoindentation of ZnO:Ga and ZnO:In Ceramics

To study the differences in the mechanical behaviour, it was necessary to carry out measurements on individual grains at different loads. Under low loads, the hardness values in the individual grain by the movement of structural defects are determined. Under higher loads when the size of deformation zone exceeds the size of grain, the hardness is affected by properties of GBs [11], [12], [16]. As it is known, according to the Berkovich hardness formula  $H = 2.092 \frac{P}{a^2}$ , where  $P$  – load,  $a$  – side of Berkovich indenter imprint, indentation

depth  $h$  is calculated as  $h = a/7.7$ . The size of the deformation zone around the imprint can be estimated as  $t = n \cdot a$ , for oxide systems a value of the coefficient  $n$  of 1.5 can be assumed [12].

Figure 2 shows the hardness and modulus of elasticity vs indentation depth for ZnO:Ga and ZnO:In ceramics. Results showed the presence of hardness size effect for both ceramics. However, this effect is expressed in a different range of indentation depths compared to ZnO single crystal [14], [15]. In order not to take into account

the influence of both size effect and nano-heterogeneity of the relief, the results

starting from a depth of 50–100 nm will be considered.

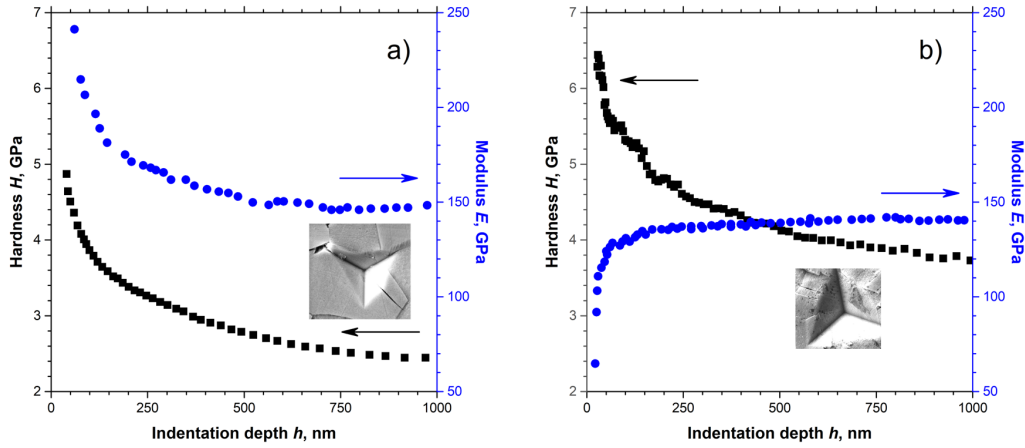


*Fig. 2.* Hardness,  $H$  (■) and modulus of elasticity,  $E$  (●) vs. indentation depth: ZnO:Ga (a) and ZnO:In (b) ceramics. The inserts show SEM images of indentation induced cracking at large loads: (a) in ZnO:Ga and (b) in ZnO:In.

In the ZnO:Ga ceramics (Fig. 2a) at depth of 100 nm, the deformation zone of 1.16  $\mu\text{m}$  is smaller than the grain size (3–8  $\mu\text{m}$ ). The hardness values inside the grain are around 4.0–4.5 GPa ( $\pm 0.3$  GPa), which is consistent with those for the single crystal or within grain in undoped ZnO ceramics. At depth of 600 nm when deformation zone is more than 8.0  $\mu\text{m}$  and more grains become included into the deformation process, the hardness values decrease to 2.5 GPa. As it can be seen from the inserts in Fig. 2a, the drop in the hardness values is accompanied with the development of cracks (with length  $C \geq 10 \mu\text{m}$ ) around the imprint, indicating the brittleness of GBs in the ZnO:Ga ceramics. At the same time, the average value of modulus of elasticity at the depth of 100–250 nm inside the grains ( $175 \pm 2$  GPa) is higher compared to that for undoped ZnO single crystal, where  $E = 140$ –144 GPa [14]. As it is known, the elastic modulus is almost insensitive to the grain size, but it is rather sensitive to the presence

of additive elements and compounds in the microstructure [10]. Therefore, an increase in the elastic modulus indicates a change in the structural-phase state of the grain, which can be associated with the presence of a ZnO-based solid solution with a low concentration of the ZnO(Ga) compound. This is indirectly confirmed by the data on the modulus of elasticity of gallium oxide (170 GPa) obtained in [16]. The presence of gallium inside the grain is also consistent with the data of ZnO:Ga ceramic microstructure given above where, as seen from Fig. 1b, c, gallium refines grains without GBs modification.

The loading experiment for the ZnO:In ceramics was carried out both at the centre of a large grain with size of 8–12  $\mu\text{m}$  and near GBs. As it is apparent from Fig. 2b, the hardness values at the depth of 100 nm when the deformation zone is inside an individual grain are 4.5–5.0 GPa and slowly decrease to the values of 4.2 GPa when approaching the GBs at the indentation depth of 400–500 nm. Thus,

the influence of GBs on the hardness in this case is not high compared to that of the ZnO:Ga ceramics. Moreover, at the depth of 1000 nm, where the deformation zone of 11.5  $\mu\text{m}$  considerably exceeds the grain size, the hardness value of 3.8 GPa remains higher compared to the ZnO:Ga ceramics. The modulus for the ZnO:In ceramics did not have high values within the grains remaining at the level of 140 GPa.

To elucidate the features of the GBs, similarly to the above-mentioned measurements for the centre of the grain, NI measurements were performed directly near the GBs: 1.5  $\mu\text{m}$  away from a randomly selected GB. In this case, the hardness values were around 3.2 GPa and they generally remained constant at the depth of 2000 nm, exhibiting no signs of long brittle cracks around the imprint. Only a narrow crack with the length  $C = 3.0 \mu\text{m}$  could be seen (Fig. 2b).

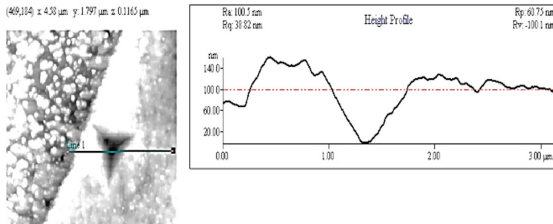


Fig. 3. AFM topography image and height profile across the imprint of the Berkovich pyramid located close to a GB in the ZnO:In ceramics.

To confirm this hypothesis, let us analyse the loading curves for two cases: (i) when deformation is localised within grains and (ii) when deformation occurs near GBs. The loading – unloading curves (Fig. 4) revealed differences for these two groups. The calculated work of plastic deformation during NI, according to [19], shows a

SEM images (see insets in Fig. 2a, 2b) and the data obtained above made it possible to estimate the values of fracture toughness by indentation ( $K_{IC}$ ) for investigated ceramics using the formula  $K_{IC} = 0.016 (E/H)^{1/2} P/C^{3/2}$  [17], where  $E$  – modulus,  $H$  – hardness,  $P$  – load,  $C$  – crack length. Assessments received were:  $K_{IC} = 1.12 \text{ MPa m}^{1/2}$  and  $K_{IC} = 2.5 \text{ MPa m}^{1/2}$  for ZnO:Ga and for ZnO:In, respectively. Thus, indentation toughness of the ZnO:In ceramics is higher than that of ZnO:Ga ceramics, which is due to the peculiarities of the GBs properties.

To visualize the unusual behaviour of GBs in the ZnO:In ceramics, measuring the height profile across the imprint placed directly near the GBs was performed.

As it is apparent from Fig. 3, the height of the piled-up material near the GB is double the height on the opposite side, which indicates plastic deformation and stress relaxation at GBs in the ZnO:In ceramics.

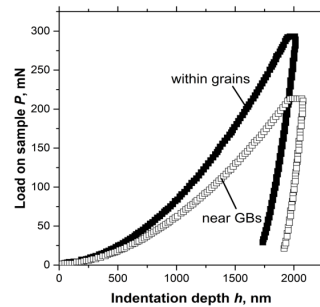


Fig. 4. Loading – unloading curves at indentation on grain and near the grain boundary vs. indentation depth for the ZnO:In ceramics.

greater value near the GBs in comparison with the bulk of the grain: 81 % and 91 %, respectively. Thus, the addition of indium oxide leads to the appearance of some GB plasticity in ZnO:In ceramics. The influence of dopants on the GBs properties in ZnO varistors is well known and is related to the segregation of the doping metallic elements

at GBs [20]. This is the so-called “metallization” phenomenon, which is unwanted in varistors because it greatly reduces the electrical resistance of the ZnO ceramics. In the

### 3.3. Fractography and EDS Data

Fracture surfaces of the samples were investigated using SEM and EDS methods.

case of mechanical properties, the presence of indium at GBs is favourable, as it eliminates the GB brittleness.

Data of fracture mode of undoped, ZnO:In and ZnO:Ga ceramics are presented in Fig. 5.

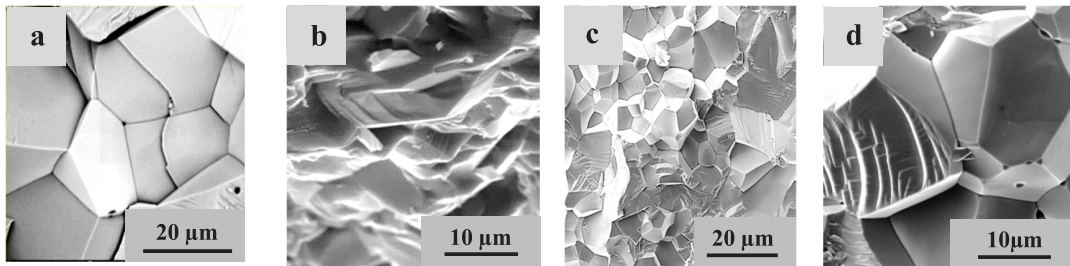


Fig 5. SEM images of the fracture surfaces in undoped (a), In-doped (b) and Ga-doped (c, d) ZnO ceramics.

As it is apparent from the SEM images, the undoped ZnO ceramics (Fig. 5a) mainly exhibits brittle intergranular fracture. Cracks and micropores are visible. The introduction of indium completely changes the mechanism of ZnO ceramics fracture. As seen in Fig. 5b, the ZnO:In ceramics has transcrystalline fracture mode. Stretched grains and the contours of GBs without micropores or crack were possible to detect.

On the contrary, the fractographs of the ZnO:Ga ceramics demonstrate heterogeneous microstructure and brittle intercrystalline fracture mode (Fig. 5c, d). Small micropores with size of 0.1–0.2 μm on the GBs and in the grains are present in this material. This result confirms the impossibility of vacancy dissolution of pores in the case when the size of pores is much less than the distance (5–8 μm) between sources (in grains) and sinks of vacancies on GBs [20]. The rounded shape of micropores in the grain and triangular shape at the triple joints of GBs indicate the role of micropores as vacancy sinks [21].

The EDS measurements were conducted on the fracture surfaces to determine the relative ratio of Zn/O in the grains and at the GBs for Ga- and In-doped ZnO ceramics (Fig. 6). Gallium was not detected due to its low concentration and low atomic number, which is 31, compared to indium number, which is 49. EDS data for ZnO:In ceramics clearly demonstrate at GBs (Fig. 6b).

Let us consider the obtained EDS values for ceramics in detail compared to single ZnO crystal where Zn/ O ratio is 49.94:50.06 at.%

For ZnO:In ceramic, as it is seen in Fig. 6a, grains in core are enriched with oxygen, but amount of Zn is reduced; in places with numerous GBs (Fig. 6b), the GBs are enriched with Zn and indium but depleted in oxygen.

In the ZnO:Ga ceramics (Fig. 6c), grains are enriched with Zn and depleted with oxygen, but in the grain groups, where the ratio was 47.02:52.98 (at.%), GBs were enriched with oxygen but depleted with Zn.



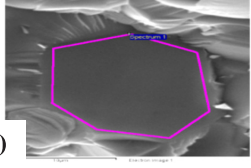
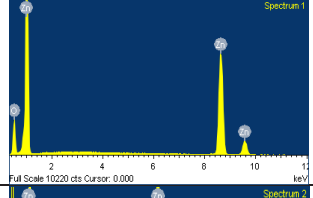
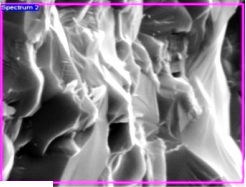
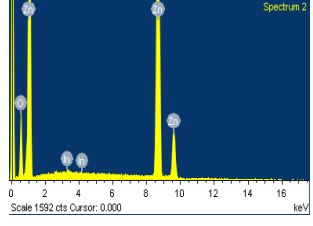
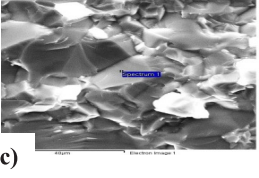
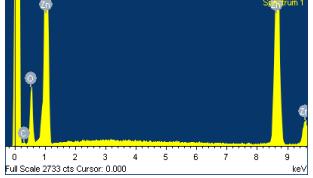
Structure	EDS spectra	Elements, at%						
 <p>a)</p>		<p>ZnO :In, big grain</p> <table border="1"> <tr> <td>Zn K</td> <td>44.70</td> </tr> <tr> <td>O K</td> <td>55.30</td> </tr> </table>	Zn K	44.70	O K	55.30		
Zn K	44.70							
O K	55.30							
 <p>b)</p>		<p>ZnO :In, GBs</p> <table border="1"> <tr> <td>Zn K</td> <td>57.1</td> </tr> <tr> <td>O K</td> <td>42.6</td> </tr> <tr> <td>In K</td> <td>0.17</td> </tr> </table>	Zn K	57.1	O K	42.6	In K	0.17
Zn K	57.1							
O K	42.6							
In K	0.17							
 <p>c)</p>		<p>ZnO :Ga, grains,</p> <table border="1"> <tr> <td>Zn K</td> <td>58.47</td> </tr> <tr> <td>O K</td> <td>41.53</td> </tr> </table>	Zn K	58.47	O K	41.53		
Zn K	58.47							
O K	41.53							

Fig. 6. ZnO ceramics structure, EDS spectra and ratio of elements:  
a) ZnO:In, big grain, b) ZnO:In, places with GBs, c) grains and GBs in ZnO:Ga.

A comparison of the EDS results revealed a general regularity; namely, the location of the dopants in the microstructure was accompanied by a high content of zinc and a low content of oxygen. Therefore, the ratio Zn/O reflects also the accumulation of interstitial zinc ions under the conditions when gallium or indium substitutes zinc.

The formation of a solid solution on ZnO base is quite realistic, since the data of XRD always indicated only the wurtzite as the based structure at low impurity concentrations [3], [9]. Interstitial ions as shallow donors give rise to a number of free electrons and play an important role in the enhancement of exciton band in the luminescence spectrum of ZnO:In and ZnO:Ga ceramics [6], [7], [22]. On the other hand, interstitial zinc ions can actively participate in diffusion during ceramics sintering, which at the last stages is controlled by grain boundary diffusion [23]. This is also confirmed by the data given in [24], where the activation energies of surface ( $Q_{\text{surf}}$ ), grain boundary

( $Q_{\text{gb}}$ ) and volume ( $Q_{\text{v}}$ ) diffusion for ZnO ceramics were estimated as 158, 282 and 376 kJ mol<sup>-1</sup>, respectively. In contrast to the optical properties, the effect of indium and gallium on the structural and mechanical properties of ceramics is different, as can be seen from the results obtained. In this case, sintering and diffusion processes play an essential role in the formation of microstructure and mechanical properties.

From this point, the presence of ZnO(Ga) compound and Zn interstitial ions into grains lead to the stabilization of micropores both inside the grain and at the GBs in ZnO:Ga ceramics (Fig. 5c, d). There are no favourable conditions for healing of pores during hot pressing since the both pressure (0.2 GPa) and temperature 1150 °C (0.6  $T_{\text{m}}$ ) are incommensurably small for the required pressure (175 GPa) and for volume diffusion (0.9  $T_{\text{m}}$ ) in grains. It is also impossible to heal micropores by dissolving and emitting vacancies. As shown above (Fig. 5), they can be sinks for vacancies, which,

on the one hand, is very positive for luminescent properties, but on the other hand, it leads to increased brittleness of the ZnO:Ga ceramics.

The results obtained showed that, in contrast to gallium, indium was located at grain boundaries in the microstructure of ZnO:In ceramics (Fig. 6b). This leads to the

active participation of interstitial ions both in the sintering processes and in the modification of the GB structure. These factors contribute, as shown above, to a decrease in mechanical stresses, as well as to the appearance of some plasticity in ZnO:In ceramics.

### 3. CONCLUSIONS

---

Hot pressed indium (0.038 at.%) and gallium (0.042 at.%) doped ZnO ceramics have been studied to determine their structural and micromechanical characteristics. The use of nanoindentation, structural and EDS methods have made it possible for the first time to detect the location of Ga inside grains, indium at GBs in the microstructure, as well as their different effect on the mechanical properties of ceramics.

The ZnO:Ga ceramics is characterised by the increased values of the elastic modulus (175 GPa) inside grain, decreased hardness (2.5 GPa) near GBs and intergranular brittle fracture mode due the presence of

stable micropores. ZnO:In ceramics has modulus of elasticity and hardness values close to ZnO characteristics, transcrystalline fracture mode, increased indentation toughness and some plasticity near GBs.

The differences in the properties of the studied ceramics correlate with the location of dopants and are caused by a different behaviour of Ga and In during sintering processes.

As the main result, the ZnO:In ceramics has a greater mechanical stress relaxation potential than the ZnO:Ga ceramics. This finding is very important for the use of ZnO:In ceramics as materials for scintillator.

### ACKNOWLEDGEMENTS

---

The research has been supported by the Project ERANET RUS\_ST#2017-051(Latvia) and #18-52-76002 (Russia). The Institute of Solid State Physics, University of Latvia as the Centre of

Excellence has received funding from the European Union's Horizon 2020 Framework, Program H2020-WIDESPREAD-01-2016-2017-Teaming Phase 2 under grant agreement No. 739508, project CAMART<sup>2</sup>.

### REFERENCES

---

1. Ozgur, U., Alivov, Y. I., Liu, C., Teke, A., Reshchikov, S. ... & Morkoc, H. (2005). A Comprehensive Review of ZnO Materials and Devices. *Journal of Applied Physics*, 98, 043011.
2. Yan, T., Trinkler, L., Korsaks, V., Lu, C. Y., Berzina, B. ... & Ploog, K. H. (2020). Anisotropic Photoluminescence of Nonpolar ZnO Epilayers and ZnO/Zn<sub>1-x</sub>Mg<sub>x</sub>O Multiple Quantum Wells Grown on LiGaO<sub>2</sub> Substrate. *Optic Express*, 28 (4), 5629–5638.



3. Grigorjeva, L., Miller, D., Grabis, J., Monty, C., Kalinko, A. .... & Lojkowski, W. (2008). Luminescence Properties of ZnO Nanocrystals and Ceramics. *IEEE Transactions on Nuclear Science*, 55, 1551–1555.
4. Rodnyi, P.A., Chernenko, K.A., Gorokhova, E. I., Kozlovskii, S. S., Khanin, V. M., & Khodyuk, I.V. (2012). Novel Scintillation Material – ZnO Transparent Ceramics. *IEEE Transactions on Nuclear Science*, 59 (5), 2152–2155.
5. Wilkinson, J., Ucer, K. B., & Williams, R. T. (2005). The Oscillator Strength of Extended Exciton States and Possibility for Very Fast Scintillators. *Nuclear Instruments and Methods in Physics Research, A*, 537, 66–70.
6. Makino, T., Segawa, Y., Yoshida, S., Tsukazaki, A., Ohtomo, A., & Kawasaki, M. (2004). Gallium Concentration Dependence Of Room Temperature Near-Band-Edge Luminescence in n-Type ZnO:Ga. *Applied Physics Letters*, 85 (5), 759–761.
7. Kano, M., Wakamiya, A., Sakai, K., Yamanoi, K., Cadatal-Raduban, M. ... & Fukuda, T. (2011). Response-Time-Improved ZnO Scintillator by Impurity Doping. *Journal of Crystal Growth*, 318 (1), 788–790.
8. Muktepavela, F., Maniks, J., Grigorjeva, L., Zabels, R., Rodnyi, P., & Gorokhova, E. (2018). Effect of In Doping on the ZnO Powders Morphology and Microstructure Evolution of ZnO:In Ceramics as Material for Scintillators. *Latvian Journal of Physics and Technical Sciences*, 55 (6), 35–42.
9. Chernenko, K. A., Gorokhova, I., Erońko, S. B., Sandulenko, A., Venevtsev, I. D. ... & Rodnyi, P. (2018). Structural, Optical and Luminescent Properties of ZnO:Ga and ZnO:In Ceramics. *IEEE Transactions on Nuclear Science*, 65 (8), 2196–2202.
10. McLean, D. (1977). *Mechanical properties of metals*. Krieger Publishing Company.
11. Fisher-Cripps, A.C. (2002). *Nanoindentation*. NY. Springer.
12. Gouldstone, A., Koh, H. J., Zeng, K. Y., Giannakopoulos, A. E., & Suresh, S. (2000). Discrete and Continuous Deformation during Nanoindentation of Thin Films. *Acta Materialia*, 48 (9) 2277–2295.
13. Ivor, M., Medved, D., Vojtko, M., Naughton-Duszova, A., Marciniak, L., & Dusza, J. (2020). Nanoindentation and Tribology of ZrB<sub>2</sub> Based Luminescent Ceramic. *Journal of European Ceramics Society*, 40 (14) 4901–4908.
14. Zabels, R., Muktepavela, F., Grigorjeva, L., Tamanis, E., & Mishels-Piesins, M. (2010). Nanoindentation and Photoluminescence Characterization of ZnO Thin Films and Single Crystals. *Journal of Optical Materials*, 32 (8), 818–822.
15. Muktepavela, F., Bakradze G., & Sursaeva, V. (2008). Micromechanical Properties of Grain Boundaries and Triple Junctions in Polycrystalline Metals Exhibiting Grain Boundary Sliding at 293K. *Journal of Materials Science*, 43 (11) 3848–3854.
16. Pearton, S. J., Yang, J., Cary, P. H. IV., Ren, F., Kim, J. ... & Mastro, M., A. (2018). A Review of Ga<sub>2</sub>O<sub>3</sub> Materials, Processing, and Devices. *Applied Physics Review*, 5 (1), 011301.
17. Gong, J., Wang, J., & Guyan, Z. (2002). Indentation Toughness of Ceramics: A Modified Approach. *Journal of Materials Science*, 37, 865–869.
18. Yonenaga, I. (2005). Hardness, Yield Strength and Dislocation Velocity in Elemental and Compound Semiconductors. *Materials Transaction*, 46 (9), 1979–1985.
19. Milman, Yu. V., Galanov, B. A., & Chugunova, S. I. (1993). Plasticity Characteristics Obtained through Hardness Measurement. *Acta Metallurgica et Materialia*, 41 (9), 2523–2532.
20. Nahm, C. W., & Park, C. H. (2000). Microstructure, Electrical Properties, and Degradation Behavior of Praseodymium Oxides-Based Zinc Oxide Varistors Doped with Y<sub>2</sub>O<sub>3</sub>. *Journal of Materials Science*, 35 (12), 3037–3042.
21. Muktepavela, F., & Maniks, J. (2003). Interface Diffusion Controlled Sintering of Atomically Clean Surfaces of Metals. *Defects and Diffusion Forum*, 216–217, 169–174.

22. Kelly, J.P., & Graeve, O. A. (2012). Effect of Powder Characteristics on Nanosintering Mechanisms of Conventional Nanodensification and Field Assisted Processes. *Sintering*. Springer, Berlin, Heidelberg, 57–95.
23. Vorobyeva, N. A., Romyanceva, M. N., Forsh, P. A., & Gaskov, A. M. (2013). Conductivity of Nanocrystalline ZnO(Ga). *Semiconductors*, 47 (5), 650–664.
24. Ewsuk, K. G., Ellerby, D.T., & DiAntonio, C., B. (2006). Analysis of Nanocrystalline and Microcrystalline ZnO Sintering Using Master Sintering Curves. *Journal of American Ceramics Society*, 89 (6), 2003–2009.
25. Huang, G. Y., Wang, C. Y., & Wang, J .T. (2009). Vacancy-Assisted Diffusion Mechanism of Group-III Elements in ZnO: An Ab Initio Study. *Journal of Applied Physics*, 105 (7), 073504.